Egypt. J. Chem. **Vol. 64,** No. 4 pp. 1733 - 1742 (2021)

Egyptian Journal of Chemistry

http://ejchem.journals.ekb.eg/

Innovation and Characterization of a New Multifunctional light weight and low cost construction material from foamed rubber blend

M.M. Abdel Kader[a*], Eman O. Taha[b], A.S. El-Deeb[a],

[1] *Housing and Buildig National Research Center, Building physics Institute, Giza, Egypt*

[2] *Department of Petroleum Applications, Egyptian Petroleum Research Institute (EPRI), Nasr City 11727, Cairo, Egypt*

Abstract

New amendment in vulcanization process was used to prepare foamed rubber with enhanced physical properties other than expected and desirable thermal insulation properties. In this work the influence of foaming agent loaded NR/ SBR on thermal conductivity, density, water absorption swelling and mechanical properties was investigated. Different concentrations of foaming agent (2, 4, 6, 8, and 10 phr) were added to rubber matrix. The morphology of selected samples was characterized using scan electron microscope (SEM). An experimental investigation was carried out to obtain low cost multifunctional construction material with desirable mechanical and thermal insulation properties. The addition of foaming agent led to a decrease in thermal conductivity and density values until the concentration of 8phr after that their values slightly changed. It was also observed that mechanical properties of blends were improved with the addition of foaming agent. The optimum concentration was found to be 8phr for all measurements

Keywords: Foaming agent; rubber blend; thermal insulating; water proofing; thermal comfort

1. Introduction

The importance of efficient energy use in buildings takes the concern of scientists and engineers to develop new building systems that have the ability to reduce energy consuming in constructions. [1] R value is an indication of how well a material insulates so thermal comfort for building occupants can be achieved by using a material with convenient thermal conductivity [2]. Energy efficient buildings reduce the quantities of fusel fuel consumed and so reduce the amount of carbon dioxide and sulfur dioxide emitted to the atmosphere. Thermal insulation reduces unwanted heat loss or gain and can decrease energy requirements for heating and cooling [3]. Uses of polymeric foam in today's technology continues to grow at a rapid pace throughout the world. Numerous reasons for this growth including the lightweight, excellent strength/weight ratio, high-performance materials together with diminishing thermal conductivity, escalating costs of raw material and energy consumption [4-6]. Mechanical properties of foamed polymers change according to the additives used in the foam production improve the endurance and hardness. The inorganic-based fillers (i.e. calcium carbonate, zeolite, clay, etc.) used for developing the structure of foams [7-10]. The foams can be classified into two types based on their pore structure, the open cell structured foams and the closed cell foams. Open cell structured foams contain pores that are connected to each other and form an interconnected network which is relatively soft, such foams will be filled with whatever they are surrounded by. If filled with air, this could be a relatively good insulator, but if the open cells fill with

*Corresponding author e-mail: marwamahmoud_1211@yahoo.com.; (Marwa Abd ElKader).
Receive Date: 21 December 2020, Revise Date: 01 January 2021, Accept Date: 03 January 2021
DOI: 10.21608/EJCHEM.2021.54577.3141

water, insulation properties would be reduced. While closed cell foams do not have interconnected pores. Normally the closed cell foams have higher compressive strength due to their structures. Low conductivity gas is used to fill the high density closed cells that helps the foam to expand and fill the spaces around it. These structure foams have higher dimensional stability, low moisture absorption coefficient and higher strength compared to open cell structured foams [11-17].

Two or more polymers blended to produce a new material with improved properties that serves several industries [18, 19]. Natural rubber NR crystallizes under tension, so that it Withstands deformation and improves its strength while many other synthetic rubbers such as styrene butadiene rubber SBR-1502 does not crystallize. Blend of NR and SBR are often used in order to get desired technological properties [20]. U. Basuli et. al. employed different amounts of foaming agents in natural rubber(NR)/butadiene rubber(BR) blends to understand the foaming behavior in presence of nano-reinforcing agent. The foam rubber compounds showed much efficient energy absorbing capability at higher strains [21]. Bidyut Prava et. al. filled Epoxy resin with waste rubber crumb to optimize the strength of the composite for structural applications. Which brings about healthier and pollution free environment and conserving the resources for the succeeding generations. It gives material with low density, good stiffness, light weight and better mechanical properties [22]. N.S Ahmad Zauzi et. al. attempted to understand the foaming behavior of natural rubber foam (NRF) via microwave assisted processing using azodicarbonamide (ADC) as the blowing agent. The obtained results demonstrated that microwave can be potentially used as alternative heating to conventional oven heating in production of rubber foams [23]. Sami A. Al-Sanea *et. al.* investigated the effects of varying amount and location of thermal mass on dynamic heat-transfer characteristics of insulated building walls with same nominal resistance numerically under steady periodic conditions using climatic data of Riyadh. The authors concluded that the energy savings potential of a wall with outside insulation is superior to that with inside insulation having the same thermal mass. They found that the range of energy savings potential given by $70\% \leq \Delta \leq 99\%$ corresponds to a wide range of critical thermal mass given by 6.4 cm $\leq L_{mas,cr} \leq 29.6$ cm. They recommended that building walls should contain $L_{mas,cr}$ that corresponds to high Δ (95%) [24]. Cassandra Lafond et. al. made a Technical characterizations of five bio-based materials, they described and compared them to a common, traditional, synthetic-based insulation material, in accordance to thermal conductivity and the vapor transmission performance, as well as the combustibility of the material. They found that the properties of the bio-based insulations were not similar to the conventional expanded polystyrene on every studied aspect. Consequently, it is not possible to replace synthetic-based insulation with natural insulation without adjusting the end-use. [25]. This work aims to produce a low cost multifunctional novel construction material to produce panels that can be installed easily in Construction sites to provide thermal comfort to workers or it can be used in cavity wall for the purpose of building insulation.

2.Experimental

All materials used in this work come from Alexandria factory for tire manufacture, Egypt. The structure of these materials is as follows:

- Natural rubber (NR), with specific gravity 0.934.
- Styrene-butadiene rubber (SBR) describes families of synthetic rubbers derived from styrene and butadiene [1]. These materials have good abrasion resistance and good aging stability when protected by additives with specific gravity 0.913.
- Zinc oxide (ZnO) as activators with specific gravity 5.55–5.61.
- Stearic acid: melting point 67–69 ^{o}C; specific gravity 0.838.
- Tetramethyl thiuran disulfide (TMTD) as accelerator with specific gravity 1.29–1.31, melting point 1485 ^{o}C and orderless powder.
- Antioxidant N-isopropyl N0-cyclohexyl paraphenylene diamine (IPPD): purple gray flakes have density 1.17 g/cm3.
- Elemental sulfur (S) with fine pale yellow powder and specific Gravity= 2.04–2.06.
- Naphthenic oil, with specific gravity 0.94–0.96, viscosity 80–90 poise at 100 ^{o}C.
- Foaming agent (Azodicarbonamide) is a synthetic chemical with the molecular formula C2H4O2N4. It is a yellow to orange red, odorless, crystalline powder. Used to reduce thermal conductivity and density of rubber to obtain low cost thermal insulating material.

The samples used to perform experimental tests were prepared according to the recipe presented in Table (1). Mixing and mastication are conveniently done using two roll mills. The mixing operation was executed on two stages. The first one called master batch consist of natural rubber, activators, antioxidant, antiozonants, reinforcing agent and processed oil. The second stage is called the final batch, which consists of the previous master batch, and curing agents (Sulfur and accelerators). These materials are added at the end of process to prevent pre-vulcanization which may occur due to the elevated temperatures. The test specimens were die cut from test slabs. Vulcanization of the rubber compounds was carried out in an electrically heated uniaxial press between stainless steel plates at 150^{o}C and pressure 150 bar for a dwell time of 45 min. Samples were prepared by different shapes of molding according to the measurement types [26].

Table (1): Shows the composition of prepared samples.

Ingridents(phr*)	**samples**					
NR	50	50	50	50	50	50
SBR	50	50	50	50	50	50
Stearic acid	2	2	2	2	2	2
Zinc oxide	5	5	5	5	5	5
Foaming agent	0	2	4	6	8	10
Processing Oil	10	10	10	10	10	10
TMTD	2	2	2	2	2	2
IPPD(4020)	1	1	1	1	1	1
Sulphur	2.5	2.5	2.5	2.5	2.5	2.5

* Part per hundred parts of rubber.

Thermal Conductivity test conducted using KD2 – Pro portable thermal conductivity meter according to transient method techniques. Cubic samples of side length 5 cm at different temperature were used according to the standard .Each sample was cured for 24 hours at each temperature and then measured. Specific gravity test was conducted according to [ASTM D792] Samples were cut with dimensions (20x 20x3) mm were used [27]. Samples with dimensions (100 x 100x2) mm, soaked in water bath for 24h while weighed before and after soaking, for Water absorption test according to [ASTM D570] [28, 29]. Water tightness test was conducted according to [EN: 1928] [30]. Mechanical measurements (Tensile strength, young's modulus and elongation at break) were measured in tensile testing machine (SHIMADZU AG-X) according to [ASTM D-412-06] [31]. The hardness was determined using Shore A durometer in accordance with [ASTM D 2240-07] [32]. Compression set test (ASTM D395) [33] was performed on standard test specimen of cylindrical shape of 25 ± 0.1 mm diameter and 12 ± 0.5 mm thickness vulcanized by compression molding method. Sample was weighed by a digital balance with sensitivity 0.1 mg and then inserted in a test tube containing solvent. The blends were removed from the solvent and blotted with filter paper to remove excess solvent on the sample surface. At a given time and fixed temperature (30 ^{0}C) the blends were weighed again to calculate the different parameters of swelling measurement. Inspect S Scanning electron microscopy (SEM) with magnification up to 150000 X and resolution of 4 nm was used to indicate SEM micrographs of the polymeric composites.

3.Results and discussion

3.1. Thermal conductivity measurements:

The effect of foaming agent content on the thermal conductivity of NR / SBR blend at different temperatures is presented in Fig.1. Thermal conductivity was measured at different temperatures to indicate the stability of the samples at different temperature ranges. From this figure, it is obvious that the values of thermal conductivity show a reduction with the increase of foaming agent content due to air pores formed in the matrix. It is also evident that 8 phr has the lowest thermal conductivity value, as the thermal conductivity decreases by about 50% its value is in the range of insulating material. It is noticed that the increase of the temperature does not cause a pronounced change in thermal conductivity.as the phonon mean free path is not affected significantly at higher temperatures [34]. This means that the thermal insulation property of the samples is not affected by the variation of temperature; this will be a good application for the climate variation. The thermal conductivity of these samples is comparably less than the thermal conductivity of clay bricks, the wood concrete and concrete containing waste rubber [35, 36]. It was also seen that the thermal conductivity values is almost stable at different temperatures.

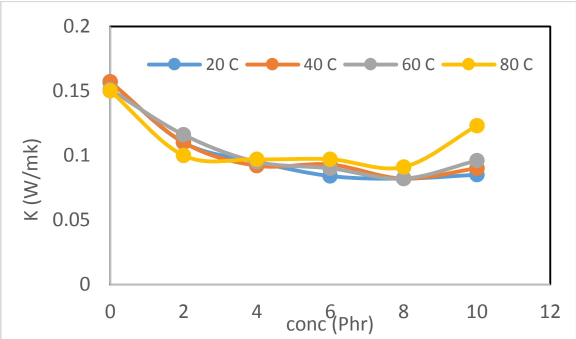

Fig. (1): The variation of thermal conductivity with foaming agent content at different temperature.

The prediction of the effective thermal conductivity (ETC) of composite or foamed composite materials is an area of interest in heat transfer applications. A substantial number of effective thermal conductivity models have been proposed, some of which have been intended for specific applications, while others have wider applicability. The simplest models of two-component composite [37, 38], would be with the materials arranged in either parallel or series with respect to heat flow, The minimum value of ETC for the series distribution in which the two phases are in layers normal to the direction of heat flow which is expressed as:

$$K_e = \frac{k_c K_d}{\phi K_d + (1-\phi) K_c} \qquad (1)$$

The maximum value of effective thermal conductivity occurs when the two phases are in layers parallel to the direction of heat flow which is given by

$$K_e = \phi K_d + (1-\phi) K_c \qquad (2)$$

The effective thermal conductivity of composites can be also calculated by the geometric mean model which assumes random distribution of phases [36].

$$k_e = k_d^{\phi} k_c^{1-\phi} \qquad (3)$$

The thermal conductivity of the solid particles is thus evaluated using the arithmetic mean model [39, 40]

$$K_e = \frac{K_U + K_L}{2} \qquad (4)$$

kU and kL can be written for two phases as follows:

$$K_U = K_c + \frac{\phi}{\frac{1}{K_d - K_c} + \frac{1-\phi}{3K_c}} \qquad (4a)$$

And

$$K_L = K_d + \frac{1-\phi}{\frac{1}{K_c - K_d} + \frac{\phi}{3K_d}} \qquad (4b)$$

Maxwell was the first to propose a theoretical model for a two phase system including homogenous spherical inclusions distributed randomly in a homogenous continuous medium (matrix) as follows [41, 42]

$$K_e = K_c\left(\frac{2K_c + K_d - 2(K_c - K_d)\phi}{2K_c + K_d + (K_c - K_d)\phi}\right) \qquad (5)$$

Another model predict ETC of the two phase systems is known as the Maxwell-Eucken model [39, 40] which assumes a dispersion of small spheres within a continuous matrix of a different component. ETC for this model is given as:

$$K_e = \frac{K_c(1-\phi) + K_d \phi \left(\frac{3K_c}{(2k_c + k_d)}\right)}{(1-\phi) + \phi\left(\frac{3K_c}{2K_c + K_d}\right)} \qquad (6)$$

The resistor model [43, 44] has been proposed to predict ETC of the two phase systems. Such phase materials have been assumed to contain cylindrical particles arranged in a regular three –dimensional cubic geometry expressed as:

$$K_e = \frac{K_c\left[(K_d - K_c)\left\{\sqrt{\left(\frac{\pi}{4}\right)}\right\}\phi^{1/2} + K_c\right]}{\left(\left[\left(1 - \left\{\sqrt{\left(\frac{\pi}{4}\right)}\right\}\phi^{\frac{1}{2}}\right)(K_d - K_c)\left\{\sqrt{\left(\frac{\pi}{4}\right)}\right\}\phi^{\frac{1}{2}}\right] + K_c\right)} \qquad (7)$$

For all mentioned theoretical models, K_e, K_c and K_d are thermal conductivities of composite, continuous-phase, and dispersed phase (filler or pores), respectively, and ϕ is the volume fraction of the dispersed-phase in matrix or porosity in the case of the foamed matrix.

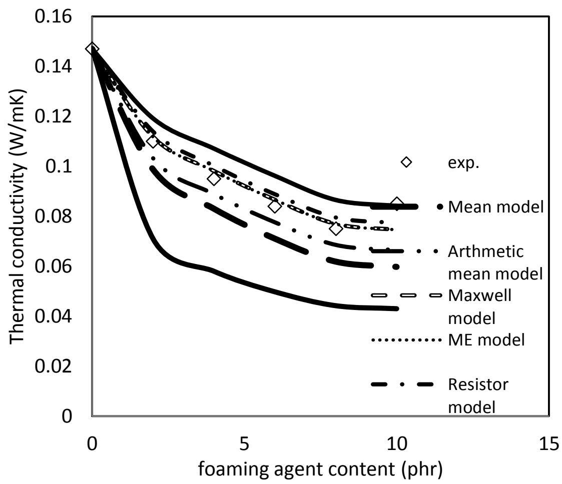

Fig. (2): Experimental and theoretical determination of thermal conductivities for foamed NR/ SBR blend.

It can be noticed from Fig. (2) That the experimental results agree with two models (Maxwell and ME) indicating the incorporation of pores are mixing of spherical and cylindrical (proved by microstructure analysis). The nearest fitted model is ME indicating the presence of spheres of the air pores formed due to addition of foaming agent leading to the decrease of thermal conductivity.

Table2: The porosity values which give good fitting for foamed rubber

Foam content (phr)	Porosity (Foamed rubber)
0	0
2	0.23
4	0.33
6	0.42
8	0.5
10	0.52

It is clear from the above table that the porosity increases with increasing foam content in rubber blend due to the increase of air pores formed.

3.2.Density

Density is an indication for the formulation process, change in microstructure, composition [45, 46], that's affect the quality of the final product. Weight reduction of some products is acceptable for product performance and economic savings. A noticeable decrease in density indicates pores existence within the product which doesn't comply with waterproofing products, while density increasing can change the polymer state approaching to crystalline state which is not compatible with waterproofing applications.

The specific gravity (ρ) was calculated according to Eq. (1) [36]

$$\rho = \frac{w_a}{w_a - w_s} x \; water \; specific \; gravity \qquad (8)$$

W_a is dry weight, and W_s is suspended in water weight.

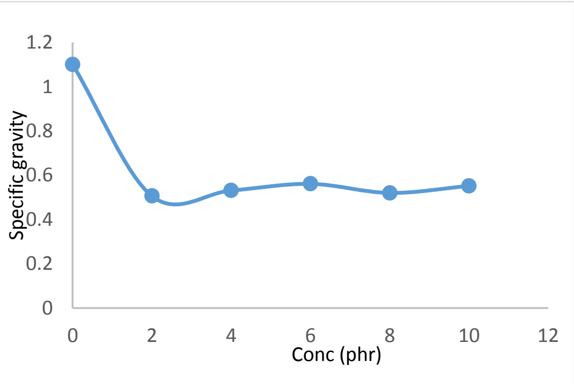

Fig. (3): The variation of specific gravity with foaming agent content.

3.3.Water absorption

Water insulation is one of the most important requirement for constructions, as moisture insulating materials protect buildings from breakdown. So it is very important to determine the water absorption percent for any construction material. The samples were immersed in water for 24h , the weight before and after immersion was recorded and water absorption present was calculated according to eq. (9) according to ASTM (D570) [29].

$$\text{water absorption } \% = \frac{m_t - m_0}{m_o} x100 \qquad (9)$$

Where, m_0 is the sample mass before immersion, m_t is the sample mass after 24hr. immersion.

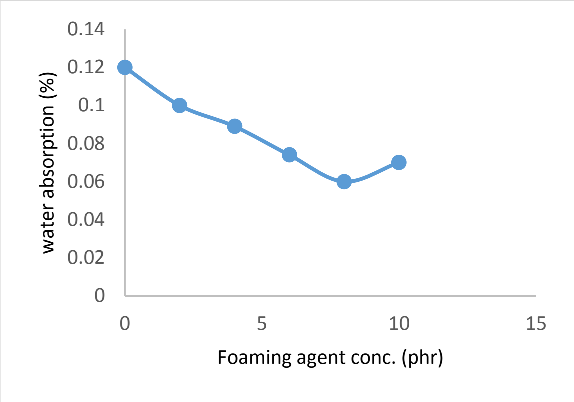

Fig. (4): The variation of water absorption present with foaming agent content.

From the above figure we can see that water absorption present decreases as the concentration of the foaming agent increases this may be due to the formation of closed pores in the matrix (illustrated in the microstructure analysis). It is clear from the above results that all samples lies in the range of water insulating materials, this considered a promising results for foamed rubber [26, 38].

3.4.*Water tightness measurements:*

All samples are exposed to water pressure of (0.6, 2, 4, 6 bars) when connected to the water tightness system, all the samples passed the test without any infiltration or cracking. While the samples considered to be accepted at 0.6bar according to EN standard [EN: 1928] [30].

3.5.Mechanical measurement:

The importance of mechanical measurements lies in its role to evaluate rubber properties and its quality, the higher the cross linking density, the larger the force required stretching the film (tensile stress), the smaller elongation at break [26], the figure below shows that the tensile strength is lower for all concentration of foaming agent than that of pure rubber blend. It was found that the elastic modulus decreases by the addition of foaming agent at 2phr then gradually increase till 8phr and then decreased again which may be due to the small amount of closed pores formed at low foaming agent concentration then closed pores gradually increased tell 8phrleading stiffness ***increase.***

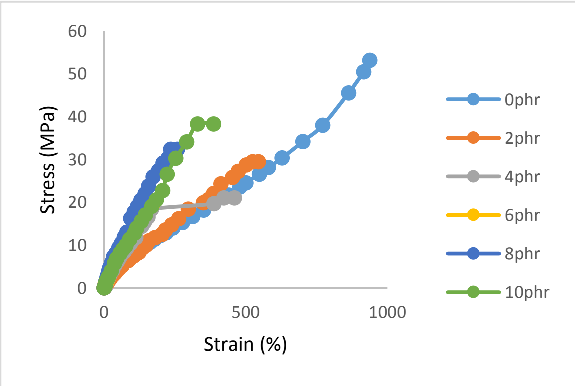

Fig. (5): Stress – Strain curve for rubber blend with different concentration of foaming agent.

Figs. (6, 7) represent the variation of tensile modulus and elongation at break versus the foaming agent loading. From these figures it can be seen that, the foamed rubber results are in the known range of reinforced rubber by some other known fillers [46].

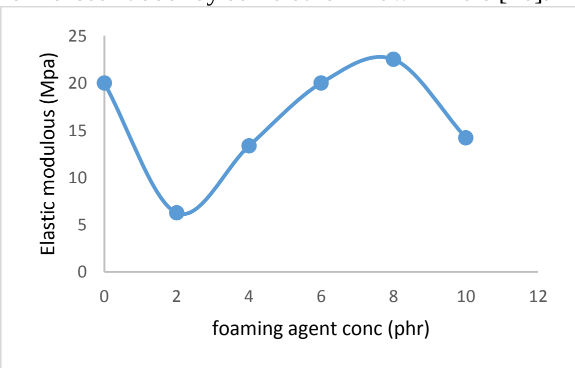

Fig. (6): Elastic Modulus for different concentration of foaming agent

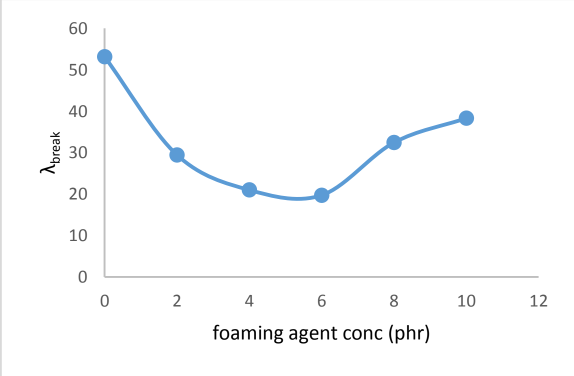

Fig. (7): Elongation at break for different concentration of foaming agent.

The crosslink densities were determined from the elastic rubbery moduli of the samples according to the rubber elasticity theory modified by Nielsen [47], from eq. (10) Where υ represents the crosslinking density which is defined as the number of moles of chains per cm3, R is the gas constant, T is the temperature in Kelvin (300K) and E is the elastic modulus obtained from the stress-stain curves. The obtained values is represented in fig. (8), this values were emphasized by the calculated values of the crosslinking densities calculated from swelling measurements as it was found that they have the same trend and order of magnitude (table 3).

$$\upsilon = \frac{E}{3RT} \qquad (10)$$

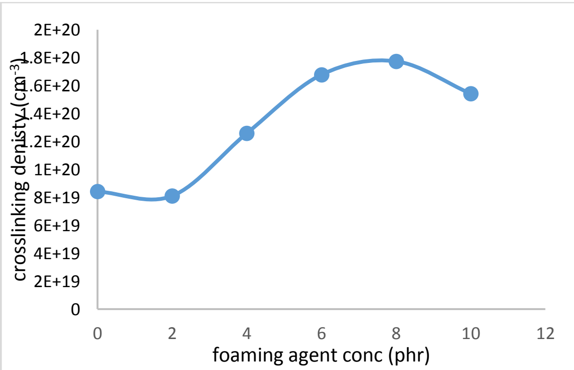

3.6.Hardness measurement:

Shore hardness is the resistance of the material to permanent deformation induced by mechanical indentation or abrasion Fig. (9) Reveals the variation of hardness as a function of foaming agent concentration. It can be observed from this figure that as the foaming agent increases which proved previously by stress strain measurements

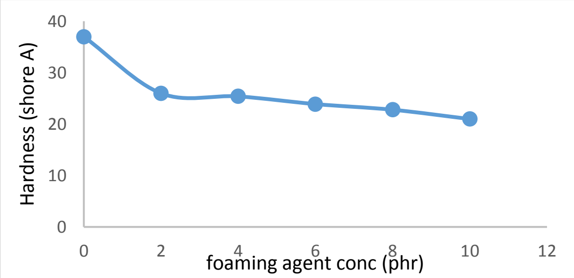

Fig. (9): variation of hardness with foaming agent loading

3.7.Compression set measurement:

The compression set % is defined by the equation:

$$C\% = \frac{t_0 - t_1}{t_0 - t_s} \qquad (11)$$

Where t_0 is the original thickness of the sample, t_1 is the thickness of the sample after removing compression, t_s is the thickness of the sample at time S. The variation of the compression set percentage (C %) as a function of filler loading for rubber blend are presented in the figure below it was proved that compression set decreases with foaming agent addition then increase with increasing the foaming agent concentration till 8phr and decreased again at 10phr which proved previously by mechanical measurements.

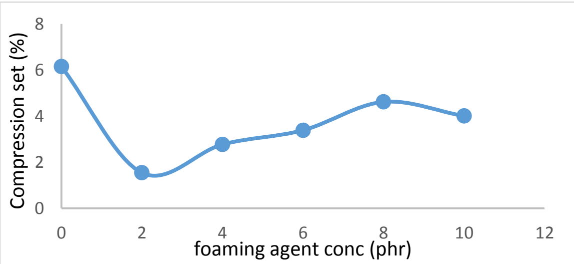

Fig. (10): variation of compression set % with foaming agent loading.

3.8.Swelling properties:

Diffusion mechanism in rubber is essentially connected with the ability of the polymer to provide pathways for the solvent to progress in the form of randomly generated voids. As the void formation decreases with filler loading, the solvent uptake also decreases (1). The degree of swelling (Q%) of the samples was calculated as follows:

$$\frac{M_t}{M_e} = \frac{4}{d}\left(\frac{Dt}{\pi}\right)^{1/2} \qquad (12)$$

Where M_t is the solvent absorbed (benzene) at time t, M_e polymer mass at equilibrium swelling, respectively, and d is the initial sample thickness. Thus, D can be calculated from the initial slope of the linear portion of a sorption curve obtained by plotting M_t/M_e versus square root of time $t^{1/2}$. [48]

This behavior could be fitted with an exponentially growth function [48]:

$$Q(t) = Q_m\left(1 - e^{-t/\tau}\right) \qquad (13)$$

Where Q_m is the maximum degree of swelling and τ is characteristic time which depends on the type and concentration of filler.

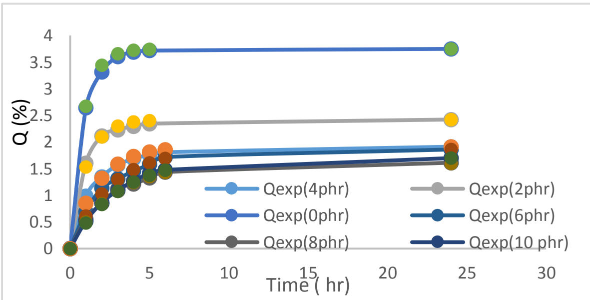

Fig. (10): Sorption curves for NR/SBR blend loaded with different foaming agent concentration.
Qexp.%:Dot symbol Qth%: solid line

All the sorption processes are similar in nature, on the contrary of expectation for foamed rubber, as the foaming agent increases the solvent uptake decreases this may be contributed to the fixed mold volume during vulcanization process which leads to formation of closed pores. Such closed pores may be responsible of reducing the solvent uptake.
Volume swelling in percentage (swelling index) was calculated using the following equation [48].

$$q - 1 = \left[\left(\frac{W}{W_o}\right) - 1\right]\frac{\rho_c}{\rho_s} \times 100 \qquad (14)$$

Where q is the ratio of swollen volume to original unswollen volume of samples, $q-1$ is swelling index, W_o is the mass of sample before swelling, W is the mass of sample after swelling for 24hr. ρ_c and ρ_s are the densities of the specimen and the solvent, respectively.

Evidently, for a given solvent, the higher the crosslinking density of the rubber the lower the degree of swelling is obtained. Then the swelling ratio is a direct measurement of the degree of crosslinking. The formation of such cross-linking is achieved by determining its density from equilibrium swelling measurements through the average molecular weight of the polymer between cross-links (M_c) according to Flory–Rehner relation [49, 50]:

$$M_c = -\frac{\rho_p V_s V_r^{1/3}}{ln(1-V_r)+V_r+\chi V_r^2} \qquad (15)$$

Where ρ_p is the density of polymer; ρp(NR/SBR) = 0.913 g/cm3, V_s is the molar volume of the solvent (benzene) = 89 cm^3/mol, χ is the interaction parameter V_r is the volume fraction of swollen rubber and given by the following relation

$$V_r = \frac{1}{1+Q} \qquad (16)$$

Where Q is defined as grams of solvent per gram of rubber hydrocarbon and calculated by

$$Q = (W - W_d)/\, W_d \qquad (17)$$

Where W_d is the deswollen weight of the sample. The crosslink density, υ_e, is defined for a perfect network as the number of elastically active network chains per unit volume and is given by [28]

$$\upsilon_e = \rho_p N_A / M_c \qquad (18)$$

Where: N_A is the Avogadro number.

Table (3): Swelling characteristic of NR/SBR blend loaded foaming agent.

Foaming agent concentration (phr)	Soluble fraction, Q (%)	V (mol/cm3)	Mc (g/mole)
0	420.698	6.93E+19	7938.116
2	271.8231	1.5E+20	3664.163
4	214.6275	2.25E+20	2445.008
6	208.6778	2.36E+20	2332.091
8	180.8153	3.02E+20	1818.492
10	190.5998	2.74E+20	2005.231

From the above table we can see that the crosslinking values have the same trend and order of magnitude of that calculated from mechanical results.

3.9.Micro structure Measurements (SEM):

Fig (11) shows the typical microstructures of 6, 8 and 10 phr foaming agent specimens respectively. It was found that the morphology of 8phr has large numbers of cosed pores which may affect the density, thermal mechanical and swelling properties of the sample.

a

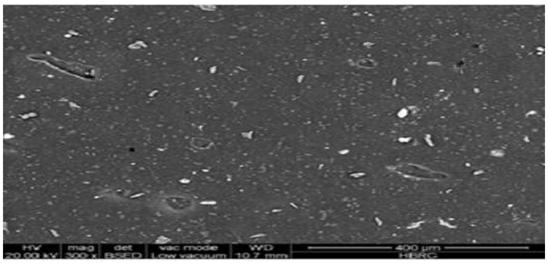

b

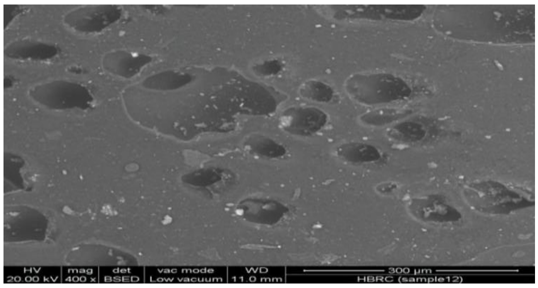

c

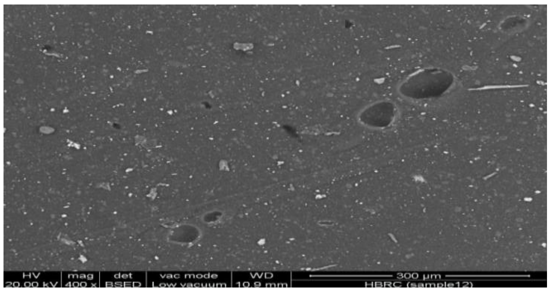

Fig (11) SEM photographs of NR loaded with:
(a) 6 phr foaming agent (b) 8 phr foaming agent
(c)10phr foaming agent.

4.Conclusion

Foamed rubber can reduce the consumption of national raw materials. By using it as an alternative multi-functional construction material. It was clear from the previous results that the thermal conductivity decreased with increasing foaming agent content which lies in the range of thermally insulating material. From the application of different thermal theoretical models it was found that The nearest fitted model is ME indicting the presence of spheres of the air pores due to addition of foaming agent leading to the decrease of thermal conductivity. It was found that the density and thermal conductivity emphasize each other and is nearly lower than that of construction building materials. The diffusion coefficient and swelling index exhibited an opposite trend to the crosslinking density. It was observed that the water absorption decreased as the concentration of foaming agent increased. Due to the poor absorption characteristic of rubber blend and incorporation of closed pores into rubber matrix. The elastic modulus had approximately the same trend as the crosslinking density. The optimum concentration for all previous measurements was found to be 8 phr which give a promising multifunctional low cost material for building application.

5.References

1. Abdel Kader M.M., Abdel-wehab S.M., Helal M.A., Hassan H.H. and Seddeq H.S., Thermal and acoustic investigation of eco-friendly building material from NR/SBR blend loaded with cement klin dust. International Journal of Advanced Research, 3 (7), 1007-1017 (2015).
2. Ristinen R.A., and Kraushaar J.J., Energy and the Environment. 2nd ed. Hoboken, NJ: John Wiley & Sons, Inc., 2006.
3. Shi C, Qian J. “High performance cementing materials from industrial slags – a review.” Resources, Conservation and Recycling 29 (2000) 195- 207 High https://doi.org/10.1016/S0921-3449(99)00060-9
4. Demir H., Sipahioğlu M., Balköse D. and Ülkü S., Effect of additives on flexible PVC foam formation. Journal of materials processing , 195, 144 (2008).
5. Zhang Z.X., Wang C., Wang S., Wen S. and Phule A.D., A lightweight, thermal insulation and excellent weatherability foam crosslinked by electron beam irradiation, Radiation Physics and Chemistry. 173, 108890 (2020).
6. Bensason S., Hiltner A. and Baer E., Damage zone in PVC and PVC/MBS blends. II. Analysis of the stress-whitened zone. Journal of Applied Polymer Science. 63 (6), (2015).
7. Chai R.D. and Zhang J., Synergistic effect of hindered amine light stabilizers/ultraviolet absorbers on the polyvinyl chloride/powder nitrile rubber blends during photo degradation. Polymer Engineering & Science. 53 (8), (2013).
8. Chen C.H. and Lo Y.W., Influences of chlorinated polyethylene and oxidized polyethylene on the fusion of rigid poly (vinyl chloride) compounds. Journal of Applied Polymer Science.74 (3), 699–705 (1999).
9. Giri R., Naskar K. and Nando G.B., Effect of electron beam irradiation on dynamic mechanical, thermal and morphological properties of LLDPE and PDMS rubber blends. Radiation Physics and Chemistry. 81 (12), 1930–1942(2012).
10. He Z.C., Zhao Z.P., Xiao S.W., Yang J.T. and Zhong M.Q., Preparation of carbon based hybrid particles and their application in microcellular foaming and flame-retardant materials. RSC Advances. 8 (47), 26563–26570 (2018).
11. Vahidifar A., Khorasani S.N., Park C.B., Khonakdar H.A., Reuter U., Naguib H.E. and Esmizadeh E., Towards the development of uniform closed cell nanocomposite foams using natural rubber containing pristine and organo-modified nanoclays, RSC Advances. 6 (59), 53981–53990 (2016).
12. Bashir M.A., Shahid M., Alvi R.A. and Yahya A.G., Effect of carbon black on curing behavior, mechanical properties and viscoelastic behavior of natural sponge rubber-based nano-composites. Key Engineering Materials. 510-511(1), 532-539, (2012).
13. Najib N., Ariff Z. M., Bakar A. and Sipaut C. S., Correlation between the acoustic and dynamic mechanical properties of natural rubber foam: Effect of foaming temperature. Materials and Design. 32, 505–511(2011).
14. Kim J-H., Koh J-S., Choi K-C., Yoon J-M., and Kim S-Y., Effects of Foaming Temperature and Carbon Black Content on the Cure Characteristics and Mechanical Properties of Natural Rubber Foams. Journal of Industrial and Engineering Chemistry. 13(2), 198-205(2007).
15. Samsudin M.S.F., Ariff Z.M., and Ariffin A., Deformation behavior of open-cell dry natural rubber foam: Effect of different concentration of blowing agent and compression strain rate. AIP Conference Proceedings 1835, 020007 (2017).
16. Yamsaengsung W. and Sombatsompop N., Effect of chemical blowing agent on cell structure and mechanical properties of EPDM foam, and peel strength and thermal conductivity of wood/NR composite–EPDM foam laminates. Composites Part B: Engineering. 40, 7, 594-600 (2009).
17. El Lawindy A.M.Y., El-Kade K.M.A., Mahmoud W.E. and Hassan H.H., Physical studies of foamed reinforced rubber composites Part I. Mechanical properties of foamed ethylene–propylene–diene terpolymer and nitrile–butadiene rubber composites. Polymer International, 51, 601–606 (2002).
18. Alsuhaiqi H.N.M., El-Gamel A.A., Khairy S.A. and Hassan H.H., Effect of compression on the electrical resistivity of EPDM/NBR rubber blends filled with different types of carbon black. Nature and Science. 12(8), (2014(.
19. Radhakrishnan C.K., Sujith A., Unnikrishnan G. and Thomas S., Effects of the Blend Ratio and Crosslinking Systems on the Curing Behavior, Morphology, and Mechanical Properties of Styrene–Butadiene Rubber/Poly (ethylene-covinyl acetate) Blends. Journal of Applied Polymer Science. 94, 827–837 (2004).
20. El-Lawindy A.M.Y., Static Deformation of Low Structure HAF Black-Loaded (SBR+NR) Rubber Blend. Polymer composite, 24, (1), 94-99 (2003).
21. Basuli U., Lee G.-B., Jang S.Y., Oh J., Lee J.H., Kim S.C., Jeon N.D., Huh Y.I., and Nah C. Foaming Behavior, Structure, and Properties of Rubber Nanocomposites Foams Reinforced with Zinc Methacrylate. Elastomers and Composites. 47 (4), 297-309 (2012).
22. Jena B.P., Nayak B.B. and Satapathy S., Physical & mechanical characterization of composites from waste tire rubber crumb. Materials today: Proceedings. 26 (2), 1752-1756 (2020).
23. Ahmad Zauzi N.S, Ariff Z.M., and Khimi S.R. , Foamability of Natural Rubber via Microwave Assisted Foaming with Azodicarbonamide (ADC) as Blowing Agent. Materials Today: Proceedings. 17, 1001–1007 (2019).
24. Al-Sanea S.A., Zedan M.F. andAl-Hussain S.N., Effect of thermal mass on performance of insulated building walls and the concept of energy

savings potential. Applied Energy. 89, 430–442 (2012).

25. Lafond C. and Blanche P., Technical Performance Overview of Bio-Based Insulation Materials Compared to Expanded Polystyrene. Buildings. 10, 81(2020).
26. El-Deeb A.S., Abdel Kader M.M. and Hassaan M.Y., Economic Polymer-based Waterproofing Membranes by Incorporation of Wastes to Form Eco-Friendly. Egyptian Journal of Chemistry. 63, (10), 3747 - 3755 (2020).
27. ASTM (D792), ASTM International, West Conshohocken, PA , Standard Test Methods for Density and Specific Gravity (Relative Density) of Plastics by Displacement. (2013).
28. Hassan H.H., Ateia E., Darwish N.A., Halim S.F., and Abd El-Aziz A.K., Effect of filler concentration on the physico-mechanical properties of super abrasion furnace black and silica loaded styrene butadiene rubber. Materials and Design. 34, 533–540 (2012).
29. ASTM (D570), ASTM International, West Conshohocken, PA,Standard Test Method for water Absorption of Plastics, (2018).
30. BS EN (1928), British Standards Institution (BSI), U.K., Flexible sheets for waterproofing. Bitumen, plastic and rubber sheets for roof waterproofing. Determination of water tightness, (2000).
31. ASTM (D 412), ASTM International, West Conshohocken, PA, Standard Test Methods for Vulcanized Rubber and Thermoplastic Elastomers-Tension, (2006).
32. ASTM (D 2240), ASTM International, West Conshohocken, PA, Shore Hardness, International standard designations, (2007).
33. ASTM D395-18, Standard Test Methods for Rubber Property - Compression Set, ASTM International, West Conshohocken, PA, (2018).
34. Regner K.T., Sellan D.P., Su Z., Amon C.H., McGaughey A.J.H. and Malen J.A., Broadband phonon mean free path contributions to thermal conductivity measured using frequency domain thermoreflectance. Nature communications. 4:1640, (2013).
35. Mohamed, M.M., Salama,T.M., Morsy, M., Shahaba, R.M.A., Mohamed, S.H. "Facile strategy of synthesizing α-MoO3−x nanorods boosted as traced by 1% graphene oxide: Efficient visible light photocatalysis and gas sensing applications" Sensors and Actuators B: Chemical (2019) 299, 126960 https://doi.org/10.1016/j.snb.2019.126960
36. Tavman I.H., Effective thermal conductivity of granular porous materials International Communications in Heat and Mass Transfer, 23 (2), 169-176 (1996).
37. Wang J., Carson J.K., North M.F. and Cleland D.J. A new structural model of effective thermal conductivity for heterogeneous materials with co-continuous phases. International Journal of Heat and Mass Transfer. 51, 2389–2397 (2008).
38. Benazzouk A., Douzane O., Mezreb K., Laidoudi B. and Quéneudec M., Thermal conductivity of cement composites containing rubber waste particles: Experimental study and modelling. Construction and Building Materials. 22(4), 573–579 (2008).
39. Khan R.B.N., and Khitab A., Enhancing Physical, Mechanical and Thermal Properties of Rubberized Concrete. In: Engineering and Technology Quarterly Reviews, 3, (1) 33-45(2020).
40. Abdolbaqia M.K., Sidik N.A.C., Mamat R., Khudhurc N.M. and Hamzah W.A.W., Experimental and numerical investigation of heat transfer augmentation using AL2O3- ethylene glycol nanofluids under turbulent flows in a flat tube. The National Conference for Postgraduate Research, Universiti Malaysia Pahang. (2016).
41. Maxwell C. and Treatise A., On Electricity and Magnetism, 3rd. Ed., 1, Ch.9 p. 1, Dover, New York (1954).
42. Altun O., Boke Y.E., Alanyali S., Numerical modeling of thermal conductivity of air-plasmasprayed zirconia with different porosity levels. Journal of Thermal Science and Technology. 31, 1, 77-84 (2011).
43. Xie J., Zhao P., Zhang C. and Jianzhong F., Measuring densities of polymers by magneto-archimedes levitation. Polymer Testing 56,308-313 (2016).
44. He, Y., Fu, J.Z., Zhao, P., Chen, Z.C., (2013) "Enhanced polymer filling and uniform shrinkage of polymer and mold in a hot embossing process" Polym. Eng. Sci. 53, 1314–1320, doi: 10.1002/pen.23379
45. Lima L.P., Juana J.C., Huang N.M., Gohd L. K., Leng F.P. and Lohd Y.Y., Enhanced tensile strength and thermal conductivity of natural rubber graphene composite properties via rubber-graphene interaction. Material science & engineering B, 246, 112-119 (2019).
46. Brinke J.W., Debnath S.C., Reuvekamp L.A.E.M and Noordermeer J.W.M. Mechanistic aspects of the role of coupling agents in silica–rubber composites. Composites Science and Technology. 63(8),1165–74. (2003).
47. Al-Sabagh A., Taha E., Kandil U., Nasr G. and Taha M.R., Monitoring Damage Propagation in Glass Fiber Composites Using Carbon Nanofibers. Nanomaterials. 6, 169 (2016).
48. M. Abdul Kader , Bhowmick A.K., Thermal ageing, degradation and swelling of acrylate rubber, fluororubber and their blends containing polyfunctional acrylates. Polymer Degradation and Stability. 79, 283–295 (2003).
49. Flory P.J. and Rehner J., Statistical Mechanics of Cross-Linked Polymer Networks II. Swelling. The Journal of Chemical Physics. 11, 521 (1943).
50. EL-Nashar D.E., Gomaa E. and Abd-El-Messieh S.L., Study of Electrical, Mechanical, and Nanoscale Free-Volume Properties of NBR and EPDM Rubber Reinforced by Bentonite or Kaolin. Journal of Polymer Science: Part B: Polymer Physics. 47, 1825–1838 (2009).
50. EL-Nashar D.E., Gomaa E. and Abd-El-Messieh S.L., Study of Electrical, Mechanical, and Nanoscale Free-Volume Properties of NBR and EPDM Rubber Reinforced by Bentonite or Kaolin. Journal of Polymer Science: Part B: Polymer Physics. 47, 1825–1838 (2009).